

Optimistic estimation on probing primordial gravitational waves with CMB B-mode polarization

Qing-Guo Huang ^{*† 1}, Sai Wang ^{‡ 2}

^{*} CAS Key Laboratory of Theoretical Physics, Institute of Theoretical Physics, Chinese Academy of Sciences, Beijing 100190, China

[†] School of Physical Sciences, University of Chinese Academy of Sciences, No. 19A Yuquan Road, Beijing 100049, China

[‡] Department of Physics, The Chinese University of Hong Kong, Shatin, N.T., Hong Kong 999077, China

Abstract

In general three frequency channels are necessary for extracting the CMB signal from the polarized dust and synchrotron emission. We make an optimistic estimation on the potential sensitivity to detect primordial gravitational waves with the cosmic microwave background B-mode polarization only, and explore how to access the thresholds for the tensor-to-scalar ratio in the well-motivated inflation models. In addition, unfortunately, considering the current limits on the tensor-to-scalar ratio, the consistency relation $n_t = -r/8$ cannot be tested due to the cosmic variance of the power spectrum of primordial B-modes which places an inevitable limit of measuring the tensor spectral index n_t , namely, $\sigma_{n_t} \simeq 1.1 \times 10^{-2}$ for $2 \leq \ell \leq \ell_{\max} = 300$.

¹huangqg@itp.ac.cn

²wangsai@itp.ac.cn

1 Introduction

The inflation model [1, 2, 3, 4, 5] has been a leading paradigm of the very early Universe in past three decades. Not only does it resolve the flatness, horizon and monopole problems in the hot big-bang theory, but also seeds primordial cosmological perturbations in the Universe [6]. The primordial tensor perturbations, predicted by the inflation, are also called primordial gravitational waves. Generically the power spectrum of primordial gravitational waves is parameterized as

$$P_t(k) = r A_s \left(\frac{k}{k_p} \right)^{n_t} \quad (1)$$

where r is called the tensor-to-scalar ratio at the pivot scale k_p , n_t denotes the tensor spectral index or the tensor tilt, A_s is the amplitude of power spectrum of primordial scalar perturbations. In the simplest version of inflation, there is a consistency relation between r and n_t , namely, $n_t = -r/8$ [7]. The tensor tilt describes the scale dependence of the tensor power spectrum.

The primordial gravitational waves have left imprints on the CMB, including temperature anisotropies and E/B-mode polarizations [8, 9, 10, 11, 12, 13, 14], which the CMB experiments have potentials to probe. Using the CMB temperature anisotropies only, Planck 2015 results (P15) [15] showed an indirect upper limit on the tensor-to-scalar ratio, namely, $r_{0.05} < 0.12$ at 95% CL. Using the B-mode data, BICEP2 & Keck Array (BK14) [16] gave the latest direct upper bound $r_{0.05} < 0.09$ at 95% CL. Combining the above two datasets with other low-redshift datasets, the upper bound becomes $r_{0.05} < 0.07$ at 95% CL [16, 17]. Using the gravitational-wave observations only, a recent constraint on the tensor tilt is $n_t = -0.76^{+1.37}_{-0.52}$ at 68% CL [18]. Further combining indirect observations on gravitational waves, this constraint becomes $n_t = -0.05^{+0.58}_{-0.87}$ at 95% CL [19]. Both constraints on the tensor tilt are consistent with a scale-invariant spectrum.

Since primordial gravitational waves have not been detected, it is worthy of exploring some well-motivated thresholds for the tensor-to-scalar ratio r . In Ref. [20], Lyth found that the tensor-to-scalar ratio is related to the excursion distance of inflaton during inflation through $|\Delta\phi|/M_p = \int_0^{N_*} \sqrt{r(N)/8} dN$, where $M_p = 1/\sqrt{8\pi G}$ is the reduced Planck scale and N is the e-folding number before the end of inflation. If r is a constant, the threshold $|\Delta\phi|/M_p = 1$ implies $r = 8/N_*^2 \simeq 2 \times 10^{-3}$. However, the current constraint on n_s from P15 [15] shows $n_s = 0.9645 \pm 0.0049$ (68% CL), and the tensor-to-scalar ratio r evolves with the expansion of the Universe during inflation, namely $-d \ln r / dN = n_t - (n_s - 1)$ by definition. For $n_s \neq 1$, the threshold for r is modified to be $r_* \simeq 2(1 - n_s)^2 / [\exp((1 - n_s)N_*/2) - 1]^2$ [21], and then $r_* \simeq 7 \times 10^{-4}$ for $n_s = 0.9645$. Furthermore, the tensor-to-scalar ratio takes the form of $r(N) = 16\alpha/(N + \alpha^{1/p})^p$ in some typical inflation models [17, 22, 23], and the threshold for r in this case is showed as the blue dashed curve in Fig. 1. For $n_s = 0.9645$, we have $r_* \simeq 4 \times 10^{-5}$. In addition, from

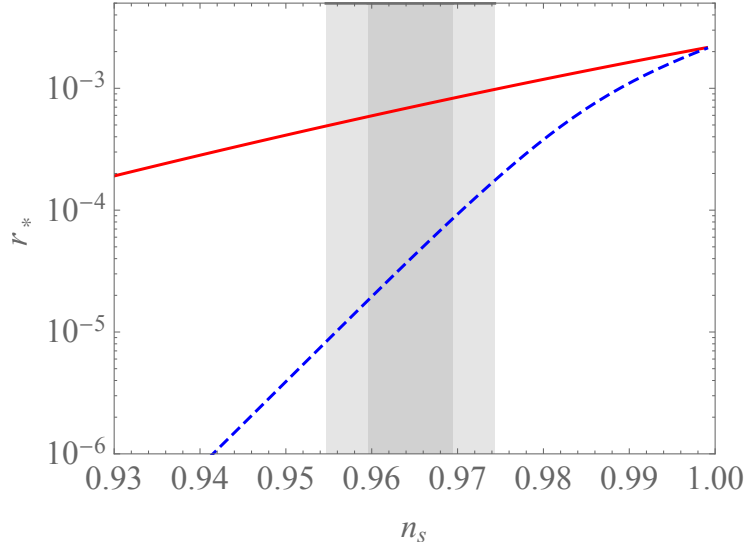


Figure 1: The threshold for the tensor-to-scalar ratio corresponding to $|\Delta\phi|/M_p = 1$. The red solid curve and blue dashed curve, respectively, correspond to the general single-field slow-roll inflation model and some typical inflation model in which $r(N) = 16\alpha/(N + \alpha^{1/p})^p$. The gray and light gray bands, respectively, correspond to the 68% and 95% limits on n_s from Planck data released in 2015 [15].

Fig. 1, the thresholds for r in both cases approach to 2×10^{-3} when $n_s \rightarrow 1$.

Two questions we are facing are how to reach these well-motivated theoretical thresholds for the tensor-to-scalar ratio and how we can test the consistency relation $n_t = -r/8$ for the simplest version of inflation model. Future improvements to the sensitivity on the primordial gravitational waves should mainly come from the CMB polarization experiments. However, the foreground radiations significantly contaminate the primordial B-mode polarizations [24, 25, 26, 27, 28, 29]. They should be taken into consideration seriously. A recent study [30] showed that the theoretically motivated $r \sim 2 \times 10^{-3}$ can be achieved by some future experiments if the instrumental white noise is reduced to $\sim 1\mu\text{K-arcmin}$ and the lensing B-modes reduced to 10%. Their forecasts are not changed significantly with respect to the previous estimates [31]. However, we found that these experiments are not sensitive enough to test the consistency relation for the simplest version of inflation in Ref. [32]. An incomplete list of other related studies can be found in Ref. [19, 33, 34, 35, 36, 37, 38, 39].

In this paper, we will explore several potential setups of the CMB polarization experiments, for which we generally consider the contaminations including foregrounds, white noise, and CMB lensing, regardless of the specific methods to reduce them. We will take these contaminations into consideration to forecast the sensitivity of these experimental setups on the primordial gravitational waves. In particular, we will explore how to reach the theoretically well-motivated thresholds for the tensor-to-scalar ratio, and see the pos-

sibility to test the consistency relation in the simplest inflation model. Our study might provide helpful guidelines for future CMB B-mode polarization observations, for example, recently funded Ali CMB project [40].

The rest of the paper is arranged as follows. In section 2, we describe our methodology in dealing with primordial B-modes, foregrounds, instrumental noise and CMB lensing. The Fisher information matrix is also introduced. In section 3, we give the results of our analysis. The conclusion and discussion are listed in section 4.

2 Methodology

In this paper we just focus on the CMB B-mode polarization, regardless the temperature anisotropy and the E-mode polarization. In this section, we demonstrate the method in dealing with various components of the CMB B-modes, as well as the technique of Fisher information matrix.

2.1 Primordial B-modes

Primordial B-modes are generated by primordial gravitational waves. Using the publicly available CAMB program package [41, 42], we can numerically calculate the power spectrum of the primordial B-modes in the linear perturbation theory, namely

$$C_\ell^{BB} \propto \int d \ln k P_t(k) [\Delta_\ell^B(k)]^2, \quad (2)$$

where Δ_ℓ^B is a transfer function and $P_t(k)$ denotes the power spectrum of primordial gravitational waves. The formula of $P_t(k)$ is given by Eq. (1). In the following, we use $\tilde{C}_\ell = \frac{\ell(\ell+1)}{2\pi} C_\ell^{BB}$ instead of C_ℓ^{BB} for simplicity.

Here the six free parameters in the base Λ CDM model are fiducially fixed to their best-fit values at the scalar pivot scale $k_p = 0.05 \text{ Mpc}^{-1}$ from Planck satellite [43, 44], i.e.

$$[\Omega_b h^2, \Omega_c h^2, 100\theta_{MC}, \tau, \ln(10^{10} A_s), n_s] = [0.02225, 0.1198, 1.04077, 0.058, 3.094, 0.9645].$$

They include the baryon density today ($\Omega_b h^2$), the cold dark matter density today ($\Omega_c h^2$), the angular scale of the sound horizon at last-scattering (θ_{MC}), the Thomson scattering optical depth due to the reionization (τ), the amplitude of scalar power spectrum (A_s), and the spectral index of scalar power spectrum (n_s). When the tensor spectral index is considered, we set a fiducial value for the tensor tilt, namely, $n_t = 0$. For the canonical single-field “slow-roll” inflation, the consistency relation is $n_t = -r/8$ [7]. Considering the current upper bounds on r , the absolute value of the tensor tilt is expected to be less than $\mathcal{O}(10^{-2})$. Thus we could set the fiducial value $n_t = 0$ for simplicity. If required, our study can be directly generalized to other fiducial values of n_t .

2.2 Foregrounds

For the foregrounds, we consider the synchrotron (S) and the Galactic polarized dust (D). One can separate them from each other in the power spectrum of CMB B-mode polarization, since they occupy very different frequency dependence. At a given frequency ν , the power spectra of them are usually given by

$$S_{\ell\nu} = (W_\nu^S)^2 C_\ell^S = (W_\nu^S)^2 A_S \left(\frac{\ell}{\ell_S} \right)^{\alpha_S}, \quad (3)$$

$$D_{\ell\nu} = (W_\nu^D)^2 C_\ell^D = (W_\nu^D)^2 A_D \left(\frac{\ell}{\ell_D} \right)^{\alpha_D}, \quad (4)$$

where the frequency dependence are denoted by W_ν^S and W_ν^D , respectively. One has

$$W_\nu^S = \frac{W_{\nu_S}^{CMB}}{W_\nu^{CMB}} \left(\frac{\nu}{\nu_S} \right)^{\beta_S}, \quad (5)$$

$$W_\nu^D = \frac{W_{\nu_D}^{CMB}}{W_\nu^{CMB}} \left(\frac{\nu}{\nu_D} \right)^{1+\beta_D} \frac{e^{h\nu_D/k_BT} - 1}{e^{h\nu/k_BT} - 1}, \quad (6)$$

where the foregrounds are normalized by the CMB blackbody $W_\nu^{CMB} = x^2 e^x / (e^x - 1)^2$ in which $x = \frac{h\nu}{k_B T_{CMB}}$, and $T_{CMB} = 2.7255\text{K}$ denotes a mean temperature of the CMB. The fiducial values of foreground parameters are listed in Tab. 1, and $A_{f_{\text{sky}}}$ denotes the

Parameters	Synchrotron	Polarized Dust
$A_{72\%}[\mu K^2]$	2.1×10^{-5}	0.169
$A_{1\%}[\mu K^2]$	4.2×10^{-6}	0.006
$\nu[\text{GHz}]$	65	353
ℓ	80	80
α	-2.6	-2.42
β	-2.9	1.59
$T[\text{K}]$	—	19.6

Table 1: A list of foreground parameters.

cleanest effective area f_{sky} in the sky and its unit is μK^2 .

The synchrotron foreground was measured by WMAP satellite [45], while the Galactic polarized dust was measured by *Planck* satellite [24]. The synchrotron is dominative below 90 GHz, while the Galactic polarized dust becomes dominative above this frequency.

The foregrounds could be cross-correlated with each other [26]. To achieve a rough estimation, we assume a correlation taking the form $g\sqrt{S_{\ell\nu_i}D_{\ell\nu_j}}$, where g denotes a correlation coefficient. In our fiducial model, we set $g = 0.5$, independent on f_{sky} , ℓ and ν . More detailed analysis is beyond the scope of this paper.

2.3 White noise

We consider the white noise which stems from the Fourier transformation of a Gaussian beam from the real space to the harmonic space. We do not consider the systematics depending strongly on specific experimental setups. The power spectrum of white noise is defined by [46]

$$\mathcal{N}_\ell = \frac{\ell(\ell+1)}{2\pi} \delta P^2 e^{\ell^2 \sigma_b^2}, \quad (7)$$

where δP denotes the instrumental sensitivity to the CMB polarizations, and $\sigma_b = \theta_{FWHM}/\sqrt{8\ln 2}$ denotes the beam-size variance. In this study, we consider several experimental settings, regardless of how to specifically implement them. The sensitivity δP is assumed to take the same magnitude for all frequency bands, but freely vary in the range $[10^{-2}, 10^2]\mu\text{K-arcmin}$. We leave this parameter to be free since we expect to study its effect on the B-modes and how to improve it. The experimental resolution θ_{FWHM} is fixed to be 5 arcmin.

2.4 Lensing residual

The gravitational weak lensing of the CMB provides another source of contamination to the detection of primordial B-modes [47]. One cannot deal with the lensing B-modes in a similar way as the foregrounds, since the lensing B-modes have the same frequency dependence as the primordial B-modes. However, one can reconstruct the lensing potential with the CMB temperature or E-modes at small angular scales, and then subtract the lensing effects from the CMB B-modes at larger angular scales [48, 49, 50, 51, 52]. This process is called delensing.

We define a parameter to describe the residual of lensing B-modes after delensing, i.e. α_L , which is independent on f_{sky} , ℓ and ν . In another word, $1 - \alpha_L$ denotes the delensing efficiency. There is no physical limit on delensing in principle. In this study, we set $\alpha_L \in [10^{-2}, 1]$ without considering how to specifically implement delensing. The lensing B-modes can be calculated with the **CAMB** program. Delensing starts to become important when the tensor-to-scalar ratio is smaller than $\mathcal{O}(10^{-2})$ if we mainly concentrate on the recombination peak of B-mode power spectra, see Fig. 2. The residual power $\delta C_\ell^{\text{lensing}} \equiv \alpha_L C_\ell^{\text{lensing}}$ of lensing B-modes could be incorporated into the power spectrum of an effective noise, i.e. $\mathcal{N}_\ell \rightarrow \mathcal{N}_\ell + \delta C_\ell^{\text{lensing}}$ [31]. In fact, the power spectrum of

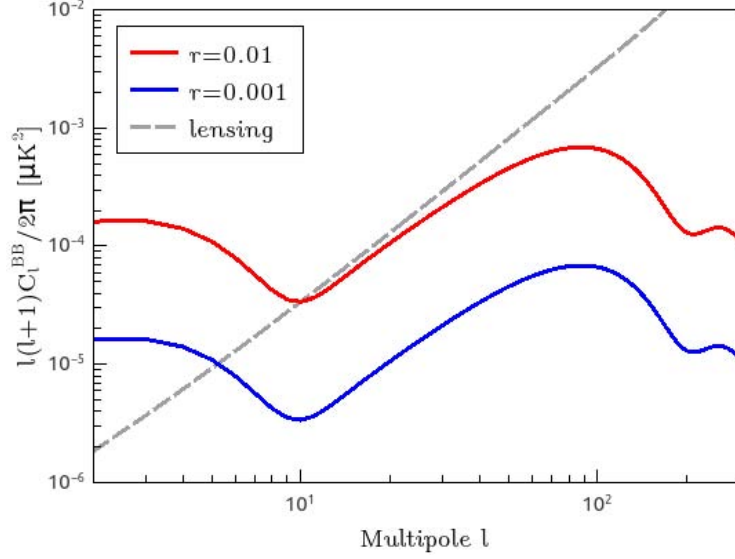


Figure 2: Primordial B-mode spectra versus lensing B-mode spectrum.

lensing B-modes ($\ell < 150$) is similar to that of the white noise with an amplitude of $4.5\mu\text{K-arcmin}$.

2.5 Fisher information matrix

In general, one could use the “component separation” (CS) method to analyze the CMB B-mode polarization data. The average log-likelihood is given by [30]

$$\langle \ln \mathcal{L}_{BB} \rangle = -\frac{1}{2} \sum_{\ell} f_{\text{sky}} (2\ell + 1) \left[\ln \det (W \mathcal{C}_{\ell} W^T + \mathcal{N}_{\ell}) + \text{tr} \left(\frac{\bar{W} \bar{\mathcal{C}}_{\ell} \bar{W}^T + \mathcal{N}_{\ell}}{W \mathcal{C}_{\ell} W^T + \mathcal{N}_{\ell}} \right) \right], \quad (8)$$

where the bar denotes all the parameters fixed to their “true” values. Here a constant term has been discarded. W describes the frequency dependence of each component of B-modes. It is a $N \times 3$ matrix with a row $(1, W_{\nu_i}^D, W_{\nu_i}^S)$. N denotes the number of frequency bands. \mathcal{C}_{ℓ} denotes the covariance matrix among three B-mode components. The Fisher matrix is defined by

$$F_{ij} = -\frac{\partial^2 \langle \ln \mathcal{L}_{BB} \rangle}{\partial p_i \partial p_j} \Big|_{\mathbf{p}=\bar{\mathbf{p}}}, \quad (9)$$

where $\bar{\mathbf{p}}$ denote the “true” values for a set of parameters \mathbf{p} . The 1σ error on a parameter p_i is given by the Cramer-Rao bound, namely, $\sigma_{p_i}^2 \geq (F^{-1})_{ii}$.

Taking into account the foregrounds, one of the aims of this paper is to explore how to reach the theory-motivated thresholds for the tensor-to-scalar ratio. Given $(\delta P, \alpha_L)$, we consider the likelihood as a function of parameters $(r, A_D, A_S, \beta_D, \beta_S, g)$. We set a fiducial value $\bar{r} = 0$. In this case the cosmic variance vanishes, and the uncertainty on r

just depends on foregrounds, noise and lensing. Thus our estimation can be viewed as an optimistic one. Considering the uncertainties, we assume the Gaussian priors for A_D , A_S , and β_S with the variance 50%, 50%, 10% and 10%, respectively. We assume a Gaussian prior for β_D with the variance 10% for $f_{\text{sky}} = 72\%$ and 50% for $f_{\text{sky}} = 1\%$, respectively. For other parameters, we do not assume priors any more. When forecasting r , we set the tensor pivot scale to be $k_p = 0.01\text{Mpc}^{-1}$ which is roughly related to $\ell \simeq 100$ in the CMB B-mode power spectrum. The 1σ uncertainty on r is obtained by marginalizing over all other parameters.

Another parameter n_t will be further added when one studies the consistency relation or equivalently the scale dependence of the tensor spectrum. In this case, the fiducial value of r can not be set to zero. One need set a non-vanishing fiducial value for r . Otherwise, both n_t and its 1σ uncertainty can take any real value. The 1σ uncertainties on r and n_t are obtained by marginalizing over all other parameters. In addition, there could be some degeneracy between r and n_t in the (r, n_t) confidence ellipse. One should choose a suitable pivot scale k_p to eliminate this degeneracy [53, 54]. In another word, one should find a suitable pivot scale such that $(F^{-1})_{rn_t} \simeq 0$. In this way, the 1σ uncertainty on r will be minimum.

3 Analysis and Results

In this section, we show our results about potential uncertainties on the tensor-to-scalar ratio r and the tensor tilt n_t due to foregrounds, noise and lensing. In particular, we predict an inevitable uncertainty on n_t due to the cosmic variance of the power spectrum of the CMB B-mode polarization.

We explore the CMB B-mode observations with three different frequency bands. We consider the following three combinations of frequency bands. The first case is given by the frequency bands (35, 90, 350) GHz, the second one (90, 220, 350) GHz and the third one (35, 45, 90) GHz. The frequency 90 GHz is CMB band, while 35 GHz and 45 GHz are synchrotron bands, and 220 GHz and 350 GHz are polarized dust bands. The frequency 350 GHz cannot be implemented on the ground, while it can be implemented in the satellite or on a balloon. Two dust/synchrotron bands can constrain the amplitude and spectral index of the dust/synchrotron power spectrum simultaneously. In addition, we consider two different sky coverage f_{sky} when we estimate the uncertainty on r . One is 72%, and the other is 1%. We consider the CMB B-mode power spectrum with $2 \leq \ell \leq 300$ for the former, while $30 \leq \ell \leq 300$ for the latter. When we estimate the uncertainties on r and n_t simultaneously, we just consider the sky coverage $f_{\text{sky}} = 72\%$.

3.1 Uncertainty on r

The polarized dust foreground has been showed having crucial impacts on constraining r [30]. Taking the polarized dust into account, we wonder whether an improvement of δP and α_L can have potential influence on constraining r . Fig. 3 shows the contours of the 1σ uncertainty on r in the $(\alpha_L, \delta P)$ plane. The left subfigures are referred to $f_{\text{sky}} = 1\%$, while the right ones $f_{\text{sky}} = 72\%$. The top subfigures are showed for the frequency bands (35, 90, 350) GHz, the middle ones for (90, 220, 350) GHz, and the bottom ones for (35, 45, 90) GHz. In each subfigure, we depict four typical contours of σ_r , namely, the red curve for $\sigma_r = 4 \times 10^{-5}$ (no display for $f_{\text{sky}} = 1\%$), the green one for $\sigma_r = 7 \times 10^{-4}$, the blue one for $\sigma_r = 2 \times 10^{-3}$, and the black one for $\sigma_r = 10^{-2}$.

From Fig. 3 we find that δP and α_L can significantly impact the uncertainty on r for a vanishing fiducial r . An improvement of δP can always bring positive influence on constraining r . However, it is not true for α_L . For $f_{\text{sky}} = 72\%$, the low- ℓ multipoles of the CMB B-modes are considered. Thus the delensing becomes essential when r is lower than the order 10^{-3} . By contrast, the low- ℓ multipoles of the CMB B-modes are not taken into account for $f_{\text{sky}} = 1\%$. Thus the delensing becomes important when r is lower than the order 10^{-2} . In fact, it is marginal to take delensing when $r \gtrsim \text{few} \times 10^{-2}$.

For $f_{\text{sky}} = 72\%$, all three experimental setups can reach the sensitivity $\sigma_r = 4 \times 10^{-5}$. In particular, the frequency combination (35, 90, 350) GHz can even reach $\sigma_r \sim \mathcal{O}(10^{-6})$. This setup covers the synchrotron band, the CMB band and the polarized dust band simultaneously. If the synchrotron band is discarded, the sensitivity becomes lower by around two times. If the polarized dust band is discarded, the sensitivity becomes lower by about one order. Our results reveal that the polarized dust foreground has more significant impact on a probe of the primordial B-modes than the synchrotron foreground does. For $f_{\text{sky}} = 1\%$, by contrast, the sensitivity on probing r becomes much lower for all three experimental setups, due to the large uncertainty on the index β_D of the polarized dust foreground and the absence of the low- ℓ multipoles of the CMB B-modes. However, the sensitivity $\sigma_r = 7 \times 10^{-4}$ may be reachable. In this case the most sensitive setup is still given by (35, 90, 350) GHz.

3.2 Uncertainty on n_t

The polarized dust radiations have significant impacts on constraining n_t [32]. For the optimistic consideration, we wonder how precisely one can measure the power spectrum of primordial B-modes and if one can distinguish it from the exactly scale-invariant spectrum. In the $(\alpha_L, \delta P)$ plane, the contours of the 1σ uncertainty on n_t are depicted in Fig. 4. The top subfigure is showed for (35, 90, 350) GHz, the middle one for (90, 220, 350) GHz, and the bottom one for (35, 45, 90) GHz. In each subfigure, we depict four typical contours of σ_{n_t} , namely, the red curve for $\sigma_{n_t} = \bar{r}/8$, the green one for $\sigma_{n_t} = \bar{r}/4$, the blue one for

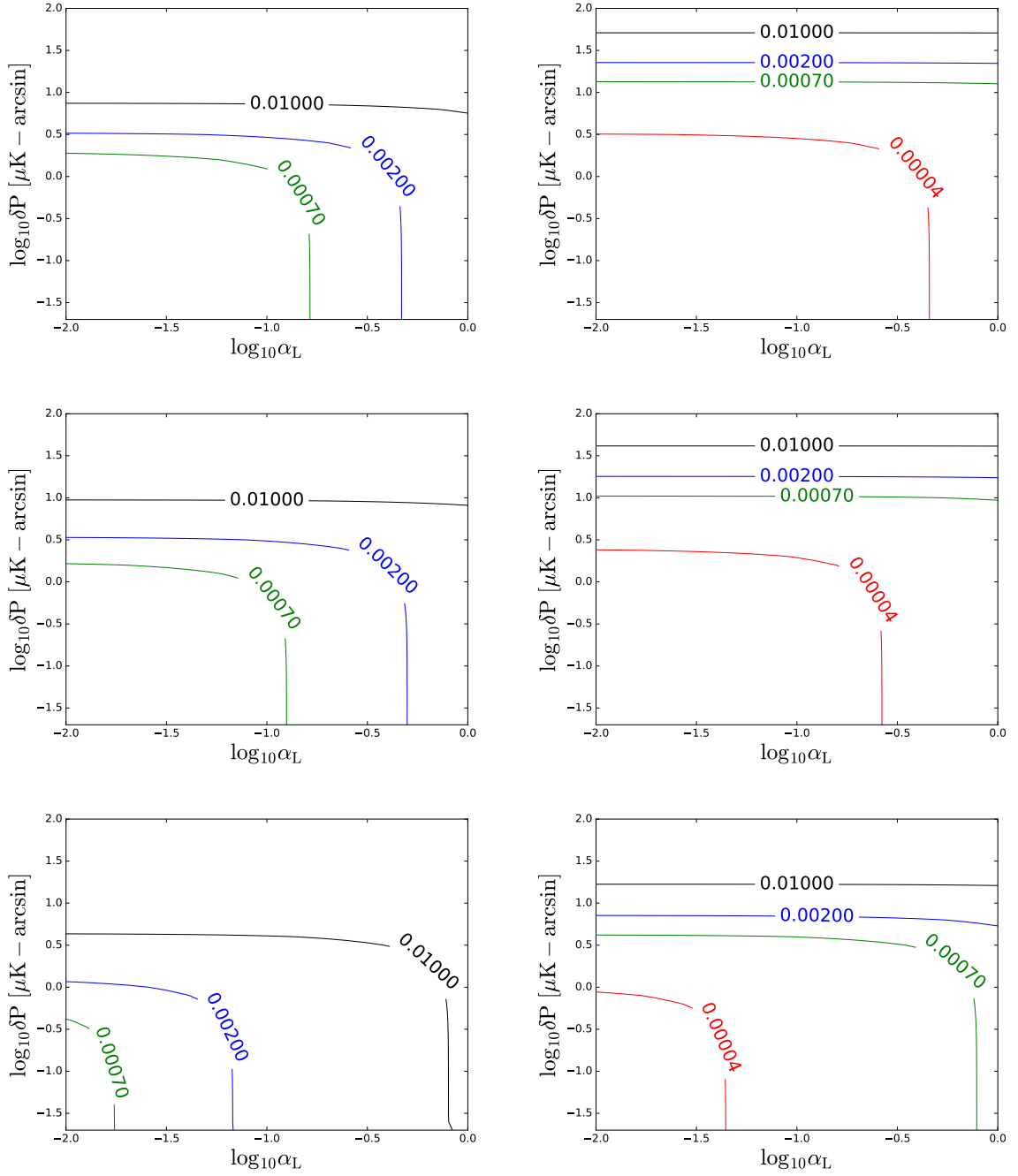


Figure 3: The 1σ uncertainty σ_r in the $(\alpha_L, \delta P)$ plane for (35, 90, 350) GHz (upper), (90, 220, 350) GHz (middle) and (35, 45, 90) GHz (lower) when $f_{\text{sky}} = 1\%$ (left) and 72% (right). We set $\bar{r} = 0$. The red curve denotes a contour of $\sigma_r = 4 \times 10^{-5}$, the green one $\sigma_r = 7 \times 10^{-4}$, the blue one $\sigma_r = 2 \times 10^{-3}$ and the black one $\sigma_r = 10^{-2}$.

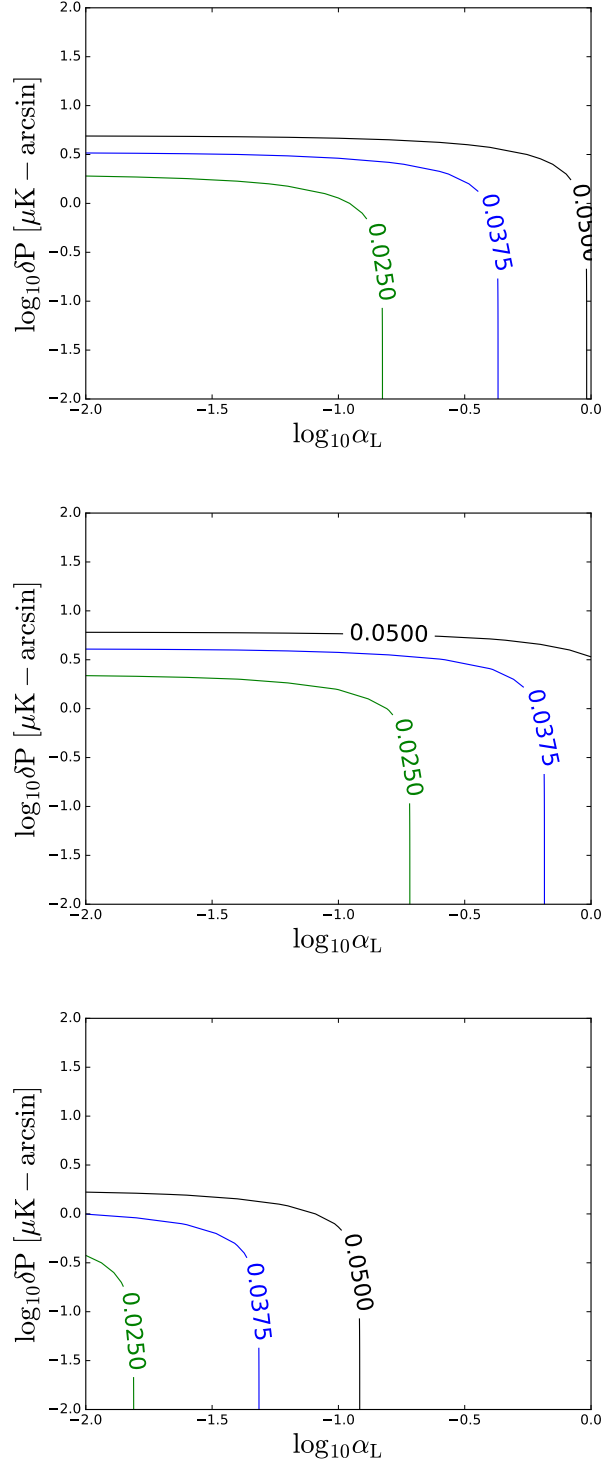


Figure 4: The 1σ uncertainty σ_{n_t} in the $(\alpha_L, \delta P)$ plane for (35, 90, 350) GHz (upper), (90, 220, 350) GHz (middle) and (35, 45, 90) GHz (lower) when $f_{\text{sky}} = 72\%$. We set $\bar{r} = 0.1$ and $\bar{n}_t = 0$. The red curve denotes a contour of $\sigma_{n_t} = \bar{r}/8$ (no display), the green one $\sigma_{n_t} = 2\bar{r}/8$, the blue one $\sigma_{n_t} = 3\bar{r}/8$ and the black one $\sigma_{n_t} = 4\bar{r}/8$.

$\sigma_{n_t} = 3\bar{r}/8$, and the black one for $\sigma_{n_t} = \bar{r}/2$. Here we set $\bar{r} = 0.1$ and $\bar{n}_t = 0$. However, the red curve does not display here since the required sensitivity has not been reached.

To be optimistic, one can reach the best sensitivity $\sigma_{n_t} \simeq 2 \times 10^{-2}$ for $\bar{r} = 0.1$. This is about two times the cosmic-variance limit showed in next subsection. Given the current constraint $r < 0.07$ at 95% CL [16, 17], one can not test the consistency relation $n_t = -r/8$ even for the most optimistic consideration in this paper.

Even though it is hopeless to test the consistency relation, the observations of CMB B-mode polarization can still place stringent constraints on n_t . For example, one may reach a sensitivity $\sigma_{n_t} \simeq 2 \times 10^{-2}$ in the optimistic consideration. Similar to r in Fig. 3, the sensitivity to n_t can be impacted significantly by both δP and α_L in Fig. 4. The setup (90, 220, 350) GHz provides the best sensitivity to n_t . The reason is that this setup can determine the parameters (i.e. A_D and β_D) of the polarized dust foreground with better precision. Therefore, a multi-band observation of the CMB B-mode polarization, better determining the polarized dust, may be helpful to learn more about n_t .

3.3 Cosmic-Variance Limit on n_t

The cosmic variance (CV), $\Delta C_\ell / C_\ell = \sqrt{2/[(2\ell+1)f_{\text{sky}}]}$ for the ℓ -th multipole, is inevitable in the CMB power spectra. It limits the accuracy and precision in determining cosmological parameters. Due to the cosmic variance, for instance, one cannot constrain r better than 0.05 with the CMB temperature anisotropies only (this amplitude will be improved by four times with the E-mode polarization only) [55]. Given present stringent constraints on r , future improvements will mainly come from the non-CV-limited B-mode polarization of the CMB. However, the CV of the B-mode power spectrum still limits the precision in measuring r with the CMB B-mode polarization only. This fact can give rise to the CV limit in determining n_t .

To find the CV limit on n_t , we consider only the primordial B-mode polarization of the CMB, disregarding the contaminations from foregrounds, noise and lensing. Thus the average log-likelihood in Eq. (8) becomes

$$\langle \ln \mathcal{L}_{BB} \rangle = -\frac{1}{2} \sum_{\ell=2}^{\ell_{\text{max}}} f_{\text{sky}} (2\ell+1) \left(\ln \tilde{C}_\ell + \frac{\bar{\tilde{C}}_\ell}{\tilde{C}_\ell} \right), \quad (10)$$

where only one frequency band is considered. Calculating the Fisher information matrix, we show the CV limit on n_t as a function of the maximal multipole ℓ_{max} in Fig. 5. For each given value of ℓ_{max} , we compute the 1σ uncertainty σ_{n_t} with the CMB multipoles of B-mode polarization from 2 to ℓ_{max} . Here we choose $29 \leq \ell_{\text{max}} \leq 300$. In principle, the CV limits with higher ℓ_{max} can also be obtained in the same approach. However, this is not necessary in the near future, since the contamination from the lensing B-mode polarization is more dominative for higher multipoles (see Fig. 2).

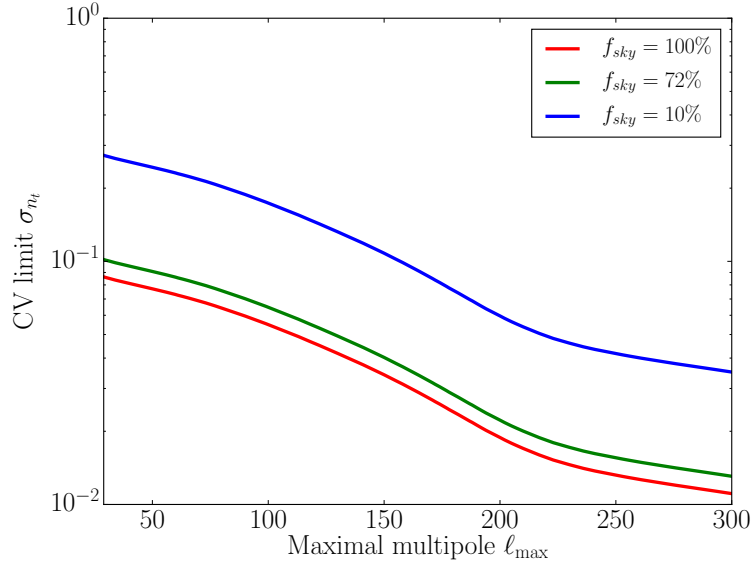


Figure 5: The CV limit on n_t versus the maximal multipole ℓ_{\max} . For a given value of ℓ_{\max} , we compute the 1σ uncertainty σ_{n_t} with CMB multipoles of B-mode from 2 to ℓ_{\max} .

The CV limit on n_t just depends on the CV of the CMB B-mode power spectrum, namely, $\Delta C_\ell^{\text{BB}}/C_\ell^{\text{BB}} = \sqrt{2/[(2\ell+1)f_{\text{sky}}]}$. For a higher ℓ , the B-mode power takes a smaller uncertainty. Therefore, σ_{n_t} decreases monotonically with ℓ_{\max} in Fig. 5. For example, in the case of full sky, our results show $\sigma_{n_t} \simeq 0.09$ for $2 \leq \ell \leq 29$ (low- ℓ multipoles) while $\sigma_{n_t} \simeq 0.01$ for $2 \leq \ell \leq 300$. In addition, σ_{n_t} becomes smaller for a larger sky coverage which covers many more multipoles of the CMB. For example, σ_{n_t} for the full sky is smaller by about three times than that for 10% sky in Fig. 5.

Considering the current constraint $r < 0.07$ at 95% CL [16, 17], it is not optimistic to distinguish the consistency relation ($n_t = -r/8$) from the scale invariance ($n_t = 0$) with the CMB B-mode only. The full-sky CV limit on n_t , denoted by the red curve in Fig. 5, cannot be crossed over definitely with the CMB B-mode polarization only. Therefore, $n_t = -r/8$ will be probably consistent with the scale invariance within the 1σ CL. To further reduce the uncertainty on n_t , one needs to supplement the CMB data with other external datasets [56]. For example, one may test the consistency relation at the 2σ CL using the 21cm line [57]. However, future observations on the CMB can still make relatively stringent constraints on n_t [32], and have potentials to rule out some models of the very early Universe, for example, the ekpyrotic universe model in which one has $n_t = 2$ [58].

4 Conclusion and Discussion

In this paper, we provided optimistic estimations on the potential sensitivity to detect the primordial gravitational waves with the CMB B-mode polarization only. In the measurement of r with three frequency bands, we found the optimistic setup to be (35, 90, 350) GHz, which covers the synchrotron, CMB and polarized dust bands simultaneously. In the most optimistic consideration, the sensitivity $r \simeq 4 \times 10^{-5}$ may be reachable for a 72% sky coverage. This sensitivity is decreased by about one order for a 1% sky coverage. In measuring n_t , we found the optimistic setup to be (90, 220, 350) GHz, including two polarized dust bands. This fact confirms the significant impact of polarized dust on measuring primordial B-modes. Our current conclusion is consistent with our previous estimation in Ref. [32].

The sensitivity to n_t is inevitably bounded by the cosmic variance of the power spectrum of primordial B-mode polarization. In this paper we also estimated the CV limit on the measurement of n_t . This limit is given by $\sigma_{n_t} \simeq 1.1 \times 10^{-2}$ for $2 \leq \ell \leq 300$. Given the current constraints on r , the consistency relation $n_t = -r/8$ can not be tested with the cosmic microwave background B-modes only. Even though challenging, however, it is still possible to discriminate some models of the very early Universe in the future.

Acknowledgments

We acknowledge the use of HPC Cluster of SKLTP/ITP-CAS. Q.-G.H. is supported by grants from NSFC (grant NO. 11335012, 11575271, 11690021, 11647601), Top-Notch Young Talents Program of China, and Key Research Program of Frontier Sciences, CAS. S.W. is supported by a grant from the Research Grant Council of the Hong Kong Special Administrative Region, China (Project No. 14301214).

References

- [1] A. A. Starobinsky, JETP Lett. **30**, 682 (1979) [Pisma Zh. Eksp. Teor. Fiz. **30**, 719 (1979)].
- [2] A. A. Starobinsky, Phys. Lett. B **91**, 99 (1980).
- [3] A. H. Guth, Phys. Rev. D **23**, 347 (1981).
- [4] A. D. Linde, Phys. Lett. B **108**, 389 (1982).
- [5] A. Albrecht and P. J. Steinhardt, Phys. Rev. Lett. **48**, 1220 (1982).

- [6] V. F. Mukhanov, H. A. Feldman and R. H. Brandenberger, Phys. Rept. **215**, 203 (1992).
- [7] A. R. Liddle and D. H. Lyth, Phys. Lett. B **291**, 391 (1992) [astro-ph/9208007].
- [8] L. P. Grishchuk, Sov. Phys. JETP **40**, 409 (1975) [Zh. Eksp. Teor. Fiz. **67**, 825 (1974)].
- [9] A. A. Starobinsky, JETP Lett. **30**, 682 (1979) [Pisma Zh. Eksp. Teor. Fiz. **30**, 719 (1979)].
- [10] V. A. Rubakov, M. V. Sazhin, A. V. Veryaskin, Phys. Lett. B **115**, 189(1982).
- [11] R. Crittenden, J. R. Bond, R. L. Davis, G. Efstathiou and P. J. Steinhardt, Phys. Rev. Lett. **71**, 324 (1993) [astro-ph/9303014].
- [12] M. Kamionkowski, A. Kosowsky and A. Stebbins, Phys. Rev. Lett. **78**, 2058 (1997) [astro-ph/9609132].
- [13] M. Kamionkowski, A. Kosowsky and A. Stebbins, Phys. Rev. D **55**, 7368 (1997) [astro-ph/9611125].
- [14] W. Hu, U. Seljak, M. J. White and M. Zaldarriaga, Phys. Rev. D **57**, 3290 (1998) [astro-ph/9709066].
- [15] P. A. R. Ade *et al.* [Planck Collaboration], arXiv:1502.02114 [astro-ph.CO].
- [16] P. A. R. Ade *et al.* [BICEP2 and Keck Array Collaborations], Phys. Rev. Lett. **116**, 031302 (2016) [arXiv:1510.09217 [astro-ph.CO]].
- [17] Q. G. Huang, K. Wang and S. Wang, Phys. Rev. D **93**, no. 10, 103516 (2016) [arXiv:1512.07769 [astro-ph.CO]].
- [18] Q. G. Huang and S. Wang, JCAP **1506**, no. 06, 021 (2015) [arXiv:1502.02541 [astro-ph.CO]].
- [19] G. Cabass, L. Pagano, L. Salvati, M. Gerbino, E. Giusarma and A. Melchiorri, Phys. Rev. D **93**, no. 6, 063508 (2016) [arXiv:1511.05146 [astro-ph.CO]].
- [20] D. H. Lyth, Phys. Rev. Lett. **78**, 1861 (1997) [hep-ph/9606387].
- [21] Q. G. Huang, Phys. Rev. D **91**, no. 12, 123532 (2015) [arXiv:1503.04513 [astro-ph.CO]].
- [22] Q. G. Huang, Phys. Rev. D **76**, 061303 (2007) [arXiv:0706.2215 [hep-th]].

- [23] J. Garcia-Bellido, D. Roest, M. Scalisi and I. Zavala, Phys. Rev. D **90**, no. 12, 123539 (2014) [arXiv:1408.6839 [hep-th]].
- [24] R. Adam *et al.* [Planck Collaboration], arXiv:1409.5738 [astro-ph.CO].
- [25] M. J. Mortonson and U. Seljak, JCAP **1410**, no. 10, 035 (2014) [arXiv:1405.5857 [astro-ph.CO]].
- [26] R. Flauger, J. C. Hill and D. N. Spergel, JCAP **1408**, 039 (2014) [arXiv:1405.7351 [astro-ph.CO]].
- [27] C. Cheng, Q. G. Huang and S. Wang, JCAP **1412**, no. 12, 044 (2014) [arXiv:1409.7025 [astro-ph.CO]].
- [28] P. A. R. Ade *et al.* [BICEP2 and Planck Collaborations], Phys. Rev. Lett. **114**, 101301 (2015) [arXiv:1502.00612 [astro-ph.CO]].
- [29] N. Aghanim *et al.* [Planck Collaboration], arXiv:1606.07335 [astro-ph.CO].
- [30] P. Creminelli, D. L. Nacir, M. Simonovic, G. Trevisan and M. Zaldarriaga, JCAP **1511**, no. 11, 031 (2015) [arXiv:1502.01983 [astro-ph.CO]].
- [31] H. Lee, S. C. Su and D. Baumann, JCAP **1502**, no. 02, 036 (2015) [arXiv:1408.6709 [astro-ph.CO]].
- [32] Q. G. Huang, S. Wang and W. Zhao, JCAP **1510**, no. 10, 035 (2015) [arXiv:1509.02676 [astro-ph.CO]].
- [33] M. Escudero, H. Ramirez, L. Boubekeur, E. Giusarma and O. Mena, JCAP **1602**, no. 02, 020 (2016) [arXiv:1509.05419 [astro-ph.CO]].
- [34] J. Errard, S. M. Feeney, H. V. Peiris and A. H. Jaffe, JCAP **1603**, no. 03, 052 (2016) [arXiv:1509.06770 [astro-ph.CO]].
- [35] M. Kamionkowski and E. D. Kovetz, arXiv:1510.06042 [astro-ph.CO].
- [36] L. Santos, K. Wang and W. Zhao, JCAP **1607**, no. 07, 029 (2016) [arXiv:1510.07779 [astro-ph.CO]].
- [37] M. C. Guzzetti, N. Bartolo, M. Liguori and S. Matarrese, arXiv:1605.01615 [astro-ph.CO].
- [38] P. D. Lasky *et al.*, Phys. Rev. X **6**, no. 1, 011035 (2016) [arXiv:1511.05994 [astro-ph.CO]].
- [39] Y. T. Wang, Y. Cai, Z. G. Liu and Y. S. Piao, JCAP **1701**, 010 (2017) [arXiv:1612.05088 [astro-ph.CO]].

- [40] Y. F. Cai and X. Zhang, *Sci. China Phys. Mech. Astron.* **59**, no. 7, 670431 (2016) [arXiv:1605.01840 [astro-ph.IM]].
- [41] A. Lewis, A. Challinor and A. Lasenby, *Astrophys. J.* **538**, 473 (2000) [astro-ph/9911177].
- [42] C. Howlett, A. Lewis, A. Hall, and A. Challinor, *JCAP* **04**, 027 (2012).
- [43] R. Adam *et al.* [Planck Collaboration], arXiv:1605.03507 [astro-ph.CO].
- [44] P. A. R. Ade *et al.* [Planck Collaboration], arXiv:1502.01589 [astro-ph.CO].
- [45] L. Page *et al.* [WMAP Collaboration], *Astrophys. J. Suppl.* **170**, 335 (2007) [astro-ph/0603450].
- [46] L. Knox, *Phys. Rev. D* **52**, 4307 (1995) [astro-ph/9504054].
- [47] A. Lewis and A. Challinor, *Phys. Rept.* **429**, 1 (2006) [astro-ph/0601594].
- [48] L. Knox and Y. S. Song, *Phys. Rev. Lett.* **89**, 011303 (2002) [astro-ph/0202286].
- [49] M. Kesden, A. Cooray and M. Kamionkowski, *Phys. Rev. Lett.* **89**, 011304 (2002) [astro-ph/0202434].
- [50] U. Seljak and C. M. Hirata, *Phys. Rev. D* **69**, 043005 (2004) [astro-ph/0310163].
- [51] K. M. Smith, D. Hanson, M. LoVerde, C. M. Hirata and O. Zahn, *JCAP* **1206**, 014 (2012) [arXiv:1010.0048 [astro-ph.CO]].
- [52] P. A. R. Ade *et al.* [Planck Collaboration], arXiv:1512.02882 [astro-ph.CO].
- [53] W. Zhao and D. Baskaran, *Phys. Rev. D* **79**, 083003 (2009) [arXiv:0902.1851 [astro-ph.CO]].
- [54] W. Zhao and Q. G. Huang, *Class. Quant. Grav.* **28**, 235003 (2011) [arXiv:1101.3163 [astro-ph.CO]].
- [55] A. Lewis, “Detecting CMB tensor modes,” <http://cosmologist.info/notes/tensors.ps>
- [56] M. Hazumi, “Cosmic Microwave Background Polarization Measurements,” <http://vega.ess.sci.osaka-u.ac.jp/seminar/semiold/files/20130902Hazumi.pdf>
- [57] K. W. Masui and U. L. Pen, *Phys. Rev. Lett.* **105**, 161302 (2010) [arXiv:1006.4181 [astro-ph.CO]].
- [58] J. Khoury, B. A. Ovrut, P. J. Steinhardt and N. Turok, *Phys. Rev. D* **64**, 123522 (2001) [hep-th/0103239].